Received: 24 July 2019 | Revised: 13 January 2020 | Accepted: 24 February 2020

DOI: 10.1002/mmce.22221

INTERNATIONAL JOURNAL OF RF AND MICROWAVE COMPUTER-AIDED ENGINEERING WILEY

REVIEW ARTICLE

Design and its state-of-the-art of different shaped dielectric resonator antennas at millimeter-wave frequency band

Priya R. Meher | **Bikash R. Behera** | **Sanjeev K. Mishra**

Department of Electronics and Telecommunication Engineering, International Institute of Information Technology Bhubaneswar, Bhubaneswar, Odisha, India

Correspondence
Priya R. Meher, Department of Electronics and Telecommunication Engineering, International Institute of Information Technology Bhubaneswar, Bhubaneswar, Odisha, India.
Email: priyaranjan.meher@ieee.org

Abstract

This review article provides an extensive literature survey on the research progress of dielectric resonator antenna (DRA) at millimeter-wave frequency band that includes concepts of DRAs, their empirical formulae and design methodologies for different shaped DRAs at 60 GHz frequency band. The different shaped DRAs such as cylindrical, rectangular, hexagonal, and octagonal at 60 GHz are designed, simulated and analyzed using CST microwave studio solver. The −10 dB impedance bandwidth of cylindrical, rectangular, hexagonal, and octagonal DRAs are 52.7 to 62.8 GHz, 57 to 62.2 GHz, 55.8 to 64.2 GHz, and 54.2 to 63.5 GHz, respectively. The idea behind getting broad impedance bandwidth is due to use of double-layer substrate with different permittivity ($\varepsilon_{r1} = 4$ and $\varepsilon_{r2} = 11.9$). Empirical formulae are deduced for hexagonal and octagonal DRA, by studying the analogy of dielectric resonator geometry. Consequently, the mode of different shaped DRAs, that is, HEM_{111} and TE_{111} are investigated by the electric field and magnetic field distribution. With these analysis, a comprehensive research review over the period of the last two decades is carried for investigating various techniques, targeted to realized gain, circular polarization, and impedance bandwidth. Along with these analysis the state-of-the-art at different shaped DRAs at mm-wave frequency band are also reported.

KEYWORDS

circular polarization, dielectric resonator antenna, millimeter-wave frequency, mode analysis, wideband antenna

1 | INTRODUCTION

The realization of dielectric resonator antennas (DRAs) started back in the period of 1980s and with its proactiveness such as high efficiency, low metallic loss, wideband characteristics, and shape flexibility; it became an emerging solution for modern wireless communication systems.[1] It is suitable for the microwave and mm-wave communication because of its constructional features such as the absence of metallic part resulting in less conduction losses as compared to that of typical planar antennas. The research on dielectric resonator (DR) begins long back in the era of 1930s, wherein 1939, the DR was conceptualized by Richtmger,[2] showing that the suitable object made of the dielectric material can function as an electrical resonator for high-frequency oscillation and that to which, it can work as energy-storing device. In addition to that, he developed the theory of resonator; computed its resonant frequency and thereby explained about the losses of DR. Later, in 1983, Long et al[3] have introduced cylindrical dielectric cavity antenna, consisting of leaky waveguide model (magnetic

conductor model) of the dielectric substrate. From that period, many advances have occurred in the field of DRA for wireless communication and its development is still continuing at a faster pace, with new intuitiveness. Some of the basic DRAs such as cylindrical, rectangular, and hemispherical, researchers have deeply investigated in terms of theoretical analysis and mathematical modeling with different modes characteristics. In spite of these shapes, the mathematical investigation of other shapes DRAs are limited. To fulfill the above demand, the authors have investigated hexagonal and octagonal shape DRAs along with cylindrical and rectangular DRAs (RDRAs) in terms of mathematical modeling and their mode characteristics.

Conventionally, out of the different types of antenna, microstrip antenna is popularly used due to low profile and easy to fabricate,[4-6] but there are certain constraints, which makes their usage limited like narrow bandwidth, maximum surface waves, low gain, and antenna efficiency. As operating frequency increases drastically toward mm-waves (30-300 GHz), the conduction losses also increase and radiation patterns become scattered, thereby results in poor antenna efficiency. So, the microstrip patch antenna is unable to perform well in this scenario. To overcome that, DRAs becomes an optimum choice of suppressing these disadvantages of metallic antennas at mm-waves and beyond. This is mainly attributed to the fact that DRAs do not suffer from conduction losses and characterize by high radiation efficiency, when the feed is excited properly. For bringing a new horizon, an overview of basic shapes DRAs[7-22] and a complete state-of-the-art for mm-wave DRAs[23-58] are presented, as a comparative focus. Then, a working methodology in the form of design, simulation, and analysis of basic shaped DRAs[59] at 60 GHz mm-wave frequency band are reported. The outline of this review article is shown in Figure 1. The review article is comprised of the following sections: Section 2 deals with an overview of DRAs. A complete state-of-the-art and literature survey on DRAs at mm-wave are reported in Section 3. For its practical realization and consideration of trade-offs, different shapes such as cylindrical, rectangular, hexagonal, and octagonal DRAs are designed, simulated, and analyzed at 60 GHz. Among these shapes, empirical formulae for hexagonal and octagonal DRA are deduced and validated. These findings are summarized in Section 4. DR materials and potential applications at mm-wave DRAs are reported in Section 5. Finally, conclusion is presented in Section 6, followed up by references.

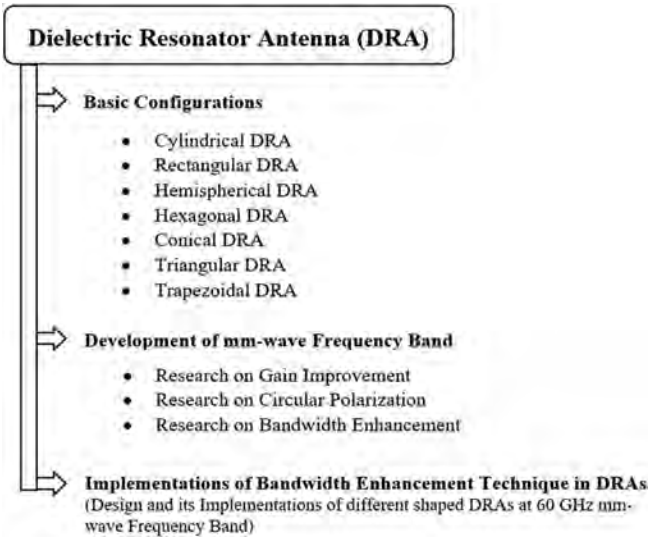

FIGURE 1 Outline of the review article

2 | AN OVERVIEW OF DRAs

DR is the heart of DRAs that capable of radiate energy into free space at a certain frequency when the source is excited appropriately. Generally, DRA is a three-layered structure consisting of DR having different permittivity materials,[7] substrate and ground plane. In 1939, DR was used as an energy-storing device but later in 1983, it was capsulated beyond energy-storing device (energy radiator), where the behavior of the material depends on Q-factor and radiation of energy in free space. The concept behind both energy storing and energy radiator describes the working principle of electromagnetic waves and the formation of standing waves inside of the DRA. When the DR is excited at suitable radiating modes, the standing waves propagate from the radiator wall and starts radiating into free space. The walls of the resonator are partially transparent to EM waves that allow them to radiate into the free space.[8] The shape of the block, overall physical dimensions and permittivity of DR material determine the resonant frequency of DRA.

2.1 | Basic configurations

Since the DRAs are available in different shapes: cylindrical DRA (CDRA),[9-11] rectangular DRA,[12-14] hemispherical DRA,[15-17] hexagonal DRA,[18] conical DRA,[19] triangular DRA,[20,21] and trapezoidal DRA[22] as shown in Figure 2. The complete performative analysis of various antenna's characteristics such as operative frequency, realized gain, antenna efficiency, modes of excitation, and polarization diversity are studied and tabulated in Table 1. For understanding the logic behind the dimensions of DR, empirical formulae/transcendental equations for different shapes of DRAs are reported.

Chowdhury et al[9] have investigated about wideband circularly polarized CDRA, consists of a cylindrical DR, placed on top of a ground plane, fed by a microstrip transmission line. Circular polarization is achieved by the incorporation of two vertical microstrip lines, attached to the DR in space quadrature to generate orthogonal modes. Theoretically, to calculate the dimensions of CDRA at a particular resonant frequency (fundamental mode [$f_{\text{res, HEM11}\delta}$]), empirical formulae[8] are given as follows:

$$f_{\text{res(HEM}_{11\delta})} = \frac{6.324c}{2\pi d\sqrt{\varepsilon_{\text{eff}}+2}}\left[0.27+0.36\left(\frac{d}{4h_{\text{eff}}}\right)+0.02\left(\frac{d}{4h_{\text{eff}}}\right)^2\right] \quad (1)$$

where, ε_{eff} is the effective permittivity of the DRA, d is the diameter of the CDRA, h_{eff} is the total height (substrate and DR) of the antenna, and ε_{eff} and h_{eff} can be calculated by:

$$\varepsilon_{\text{eff}} = \frac{h_{\text{eff}}}{\frac{h_{\text{dra}}}{\varepsilon_{\text{cdra}}}+\frac{h_{\text{sub}}}{\varepsilon_{\text{sub}}}}, \quad (1.1)$$

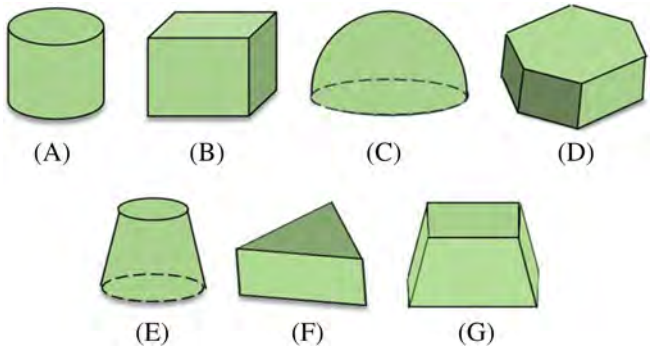

FIGURE 2 Different shapes of dielectric resonator: A, cylindrical; B, rectangular; C, hemispherical; D, hexagonal; E, conical; F, triangular; and G, trapezoidal

$$h_{\text{eff}} = h_{\text{dra}} + h_{\text{sub}} \quad (1.2)$$

where, h_{dra} is the height of DRA, h_{sub} is the height of substrate, $\varepsilon_{\text{cdra}}$ is the dielectric constant of cylindrical DR and ε_{sub} is the dielectric constant of the substrate. The advantages of CDRA[10] is ease of fabrication, design flexibility, and ability to excite different modes within the same structure, as a result of, broadside and the omnidirectional radiation pattern is observed. Mongia et al,[11] done a comprehensive review of different modes and radiation characteristics of CDRA.

Taking the same context, Moon et al[12] have investigated theoretically and practically about RDRA for dual-band PCS/IMT-2000 applications fed by a coaxial probe. Legier et al presented a paper on a calculation of resonant frequency of RDRA using dielectric waveguide model (DWM)[13] and also investigated certain facts on DWM as the usage of the semi-analytical technique of Marcatili, Knox, and Toulios model. In a comparison of both CDRA and RDRA, RDRA offers two design flexibility, that is, w/d and w/h and low cross-polarization level. The resonance frequency of the fundamental mode (TE^{x}_{111}) is calculated by Equation (2)[14]:

$$f_0 = \frac{c}{2\pi\sqrt{\varepsilon_r}}\sqrt{k_x^2+k_y^2+k_z^2} \quad (2)$$

$$k_x \tan\left(\frac{k_x d}{2}\right) = \sqrt{\left((\varepsilon_r-1)k_0^2-k_x^2\right)} \quad (2.1)$$

$$k_0 = \frac{2\pi}{\lambda_0}, k_y = \frac{\pi}{w}, k_z = \frac{\pi}{b} \quad (2.2)$$

where, k_0 is the free space wavenumber and k_x, k_y, and k_z are the wavenumber along x, y, and z coordinates, ε_r is the dielectric constant of DR, w is the width of DR, $h = b/2$ is the height of DR, b = length of the DR, and λ_0 is free-space wavelength.

TABLE 1 Comparison of basic shapes of DRAs

Ref.	DR Shape	f_o (GHz)	ε_r	G (dBi)	Eff. (%)	Feeding	Modes	Pol.
9	Cyli.	2.82-3.83	9.8	5.5	96	Microstrip	$\text{HE}^{x}_{11\delta}$, $\text{HE}^{y}_{11\delta}$	CP
14	Rect.	5.56-6.37	10.3	4.33	NM	Microstrip	$\text{TE}^{x}_{\delta 21}$, $\text{TE}^{x}_{\delta 10}$	LP
16	Hemi.	4.55	9.2	7.2	90	Coaxial	TM_{101}	LP
18	Hexa.	3-3.47	59	NM	NM	Coaxial	$\text{TE}_{11\delta}$	CP
19	Coni.	7.2-8.45	10	7.6	76-88	Aperture	$\text{HEM}_{11\delta}$	LP
21	Tria.	1.5	12	NM	NM	Coaxial	$\text{TM}_{11\delta}$	LP
22	Trap.	2.88-4.04	9.4	8.4	NM	Aperture	NM	CP

Abbreviations: Coni., conical; Cyli., cylindrical; Eff., efficiency; f_o, operating frequency (GHz); G., gain; Hemi., hemispherical; Hexa., hexagonal; NM, not mentioned; Pol., polarization; Rect., rectangular; Ref., reference; Trap., trapezoidal; Tria., triangular; ε_r, dielectric constant of DR.

Luk et al[15] have described an analysis of hemispherical DRA with a coaxial probe using green's function. Similarly, Mukherjee et al[16] presented a half hemispherical DRA with an array of slots for wideband applications with an impedance bandwidth of 1.3 GHz and realized gain of around 7.2 dBi at 4.55 GHz. Mcallister et al[17] presented a numerical validation of hemispherical DRA, as shown in Equation (3):

$$f_r = \frac{4.775 \times 10^7 \mathrm{Re}(ka)}{\sqrt{(\varepsilon_r)a}} \tag{3}$$

where, f_r is the resonant frequency, a is the radius of DRA, and ε_r is the permittivity of DRA.

In the same, Hamsakutty et al[18] have given the concept of a CP hexagonal DRA fed by a coaxial probe, that provides axial bandwidth from 3 to 3.47 GHz without using any implicit techniques. Dash et al[19] investigated conical DRA with improved gain and bandwidth for X-band applications and it is fed by aperture coupled transmission line with supersubstrate and modified ground plane for the enhancement of impedance bandwidth of the antenna. Ittipiboon et al[20] studied rectangular and triangular DRA, used as a magnetic dipole antenna element, fed by aperture coupled 50-Ω microstrip line. Both structures have shown wide impedance bandwidth (ie, >10%). Kishk examined triangular DRA and their resonant frequency can be calculated using the following transcendental equation.[21]

$$f_{mn} = \frac{c}{2\pi\sqrt{\varepsilon_r}}\left[\left(\frac{4\pi}{3L_d}\right)^2\left(m^2 + mn + n^2\right) + k_z^2\right]^{0.5} \tag{4}$$

$$k_z = \frac{\rho}{h'} \tag{4.1}$$

where, m and n are resonance frequency index, k_z is the wavenumbers in z-direction in the dielectric, c is the speed of light, ε_r is the dielectric constant of DRA and L_d is the side length of triangular DRA, h is the two times height of the DRA, and $\rho = 1$ for the fundamental DRA. Pan et al[22] investigated circular polarized trapezoidal DRA with a notch at its top, with a motive for its improvement in impedance matching from 2.88 to 4.04 GHz, respectively. Table 1 provides a comparative study about different shapes of DRAs in terms of antenna parameters along with mode analysis.

3 | A LITERATURE SURVEY ON MILLIMETER-WAVE DRAs

DRA is a suitable candidate for mm-wave communication when it is compared with the conventional metallic patch antenna.[23-58] Due to its extensive characteristics, that is, absence of metallic losses with the presence of DR, makes DRA, suitable candidate for mm-wave applications. It can also be operative for 5G applications, in which performance indices are based on spectrum selection, antenna, and propagation characteristics. The spectrum for 60 GHz mm-wave communication and its utility in terms of bandwidth in different countries[23] are reported in Table 2. The mm-wave is covering in between 30 and 300 GHz and often called as extremely high frequency. But, this frequency band has already drawn a lot of attention due to multi-gigabit communication services such as high definition (HD) multimedia interface, uncompressed HD video streaming, high-speed internet, automatic radar sensor, and wireless gigabit ethernet.[24-26] From practical realization point of view, mm-wave antennas are designed using various processes like low temperature co-fired ceramic (LTCC) process, multilayer PCB technology and die-sink electrical discharge machining (EDM) process. In LTCC process, it provides flexibility in realizing the random number of layers and cross-layer vias. Other technologies like multilayer PCB technology suffer more expenditure due to the usage of several mechanical devices, also it reduces the antenna efficiency at the high-frequency band as compared to the LTCC process. In the case of die-sink electrical discharge machining, it offers a low cost of fabrication[26] at mm-wave antennas.

Prior to it, a proper understanding needs to be persuaded for DRAs and its characteristics at mm-wave applications. With a similar context, different techniques for gain enhancement, attainment of circular polarization, and bandwidth enhancement are studied. Subsequently, in this review article, the authors have proposed different shaped DRAs at 60 GHz mm-wave applications. In addition, empirical formulae are deduced for hexagonal and octagonal shapes of DRA. Besides, mode analysis is persuaded by studying electric field and magnetic field distributions along with the

TABLE 2 Spectrum range and its bandwidth for different countries at 60 GHz mm-wave communications[23]

Sl. No	Countries	Spectrum (GHz)	Bandwidth (GHz)
1	Australia	59.4-62.9	3.5
2	China	59-64	5
3	Europe	57-66	9
4	Japan	59-66	7
5	Korea	57-64	9
6	United States	57-64	9

materials used for DR and substrate of the antenna and their potential applications toward mm-wave communications. A detailed analogy in this context is given in the next section.

3.1 | Gain enhancement techniques

The mm-wave communication systems need to be designed in such a way that, it fulfills the requirements of high-speed data rate communication. From the antenna designer's perspective, high gain with a stable radiation pattern over the entire operating band is essential for mm-wave communications. Thus, to meet the above demand, gain enhancement techniques with their evaluation matrices such as impedance bandwidth, efficiency, modes, and gain are highlighted.

Therefore, the most straightforward approach to increase the gain and radiation characteristics of the DRAs are arraying[27-31] the individual DR, surface integrated dielectric resonator antenna (SIDRA) array,[32,33] DR loaded substrate integrated waveguide[34] and substrate integrated waveguide along with aluminum frame in a backed cavity around the DR array.[35] As a result, the maximum gain is increased up to 28 dB. By introducing the multilayered DR such as rectangular DR layer having different dimensions with different permitivity[36] and z-shaped stepped DR with the same permittivity,[37] antenna gain is enhanced, but it increases the overall height of the antenna which may not be suitable for a particular application and in a scenario makes it bulky. To nullify these effects, a new hybrid structure[38,39] consisting of an annular-shaped DR coupling by a microstrip patch with aperture feed is proposed. The objective was to improve the gain of DRA with excitation of higher-order modes, that is, $HEM_{15\delta}$ inside DR. Soon, electromagnetic bandgap (EBG) structure[40] placed underneath of DRA is used to reduce the backward radiation, resulted in

TABLE 3 Gain enhancement of DRAs at mm-wave applications

Ref.	Shape	Feeding	ε_r	f_o (GHz)	Eff. (%)	Modes	Gain
27	Cyli.	SIW	7.1	25.7	74	$HEM_{11\delta}$	16.3
28	Rect.	SIW	10.2	37.7	92	NM	14.5
29	Rect.	SIG Power Splitter	NM	90-110	>95	TE^{y}_{111}	19
30	Rect.	-	2.7	26-34	79.35	NM	28
31	Rect.	SIW	2.5	29.3-35.2	76	NM	12
32	M. Rect.	SIW	10.2	32.2-35.8	NM	NM	11.5
33	M. Rect.	SIW	10.2	32.9-35.8	NM	TE^{x}_{111}	12.8
34	Rect.	Microstrip	2.23	59.5-65.9	78	TE^{x}_{111}	11.2
35	Rect.	SIW	20.5	24.8-31.2	NM	NM	18.3
36	Rect.	Aperture	10.2, 6.15, 2.2	58-68	NM	NM	11.4
37	Z-shaped	Microstrip	10.2	57.14-61.04, 64.06-69.01	95.2, 98.4	NM	11.91, 11.91
38	Annular	Aperture	10	57-65	90%	$HEM_{15\delta}$	11.9
39	Elliptical	Microstrip	10.2	55.6-65	NM	$HEM_{13\delta}$,$HEM_{12\delta}$	> 9
40	Cyli.	Aperture	10.2	~55-65	NM	NM	18
41	Rect.	Aperture	10.2	29-31.5	NM	NM	15.5
42	Rect.	Aperture	10.2	~57-67	NM	$HEM_{11\delta}$	14.26
43	Cyli.	Probe	10.2	30	NM	TM_{01}	6.1
44	Cyli.	CPW	11.9	~58.5-60.73	79.35	HEM_{111}	7
45	Rect.	Waveguide	10.2	35	95	HEM_{111}	5.51
46	Rect.	Aperture	10	55.8-65.2	NM	$HEM_{15\delta}$	13.2
47	Rect.	Microstrip	6	57-66.2	NM	NM	7.1
48	Rect.	Microstrip	20	67	96.7	$TE^{x}_{\delta 11}$	7.8
49	Rect.	Coupling	11.9	57.6-62.1, 77.1-81.2	NM	TM^{x}_{111},TM^{x}_{113}	5.1, 5.9

Note: ~ is estimated from the graph.

Abbreviations: Cyli., cylindrical; Eff., efficiency; f_o, operating frequency; M. Rect., modified rectangular; NM, not mentioned; Rect., rectangular; Ref., reference; ε_r, dielectric constant of DR.

enhancement of the radiation efficiency of DRA. Further, the frequency selective surface (FSS) substrate layer[41,42] is placed just above the DR element, resulted in the enhancement of gain. Prior, beam switching is also achieved by using cantilever based FSS.[43] A novel DRA[44] is introduced at 60 GHz mm-wave on-chip systems. It was fabricated from a single high resistivity silicon wafer via micromachining technology. This antenna has provided a number of appealing characteristics such as fabrication simplicity, high gain, low cross-polarization level, and high radiation efficiency. Keeping it in context, a planar waveguide technology-based DRA[45] is introduced to achieved high radiation efficiency over the operating frequency. Other methods like corner chamfered patch with DR,[46] square DRA with surrounded metal via to connect in between top and ground plane,[47] hybrid integrated DRA,[48] and DRA in Si-based integrated passive device (IPD)[49] are reported, to witness various methods for enhancement of gain and radiation efficiency of DRA. A detailed analogy is drawn by visualizing relevant outcomes of numerous gain enhancement techniques at mm-wave applications in Table 3.

3.2 | Circular polarization techniques

In the present scenario, circular polarization plays a crucial role in a modern wireless system at mm-wave communications. Due to its attractive features like independent antenna orientation, high reflectivity, high absorption, less multipath distortion than linear polarization (LP), it confirms the viability of circular polarization (CP). For achieving CP, various implicit techniques are considered in our review article. Starting from the chamfered both side of DR corners[46,50] two stacked dielectric rectangular strips placed upon the coupling slot with inclination angle,[35] U-shaped strip lines symmetrically etched on the different side of DR,[51] multilayered pyramidal structure DR with different permittivity,[36] and modified circular patch loaded on top of the individual DR array elements[52] are used for attainment of CP. Consequently, DR with frequency selective surface which is placed above the DRA and fed by an aperture coupled microstrip feed resulting in generation of CP radiation.[41] In addition, air gap between DRA and FSS layer together to improve CP purity as well as gain of the antenna. Other technique, that is, multi-point feed like dual microstrip feed with a loop structure with a spherical DR,[53] which can be evaluated for dual-polarization in future work of the paper. Detailed DRAs outcomes such as impedance bandwidth, CP bandwidth, modes and gain of CP techniques at mm-wave applications are reported in Table 4.

3.3 | Bandwidth enhancement techniques

A quite vast number of existing and emerging modern wireless communication systems operate over V-Band and E-Band at mm-wave communications. In this section, different techniques useful to the enhancement of the impedance bandwidth of the DRAs are summarized. Other techniques like template-based DRA array,[54] grid dielectric resonator antenna (GDRA) with substrate integrated waveguide (SIW) feeding layer,[31] modifying the geometry, that is, low profile DR with comparison of regular type (cube shape)[55] and incorporation of different feeding structure[56,57] which leads to the enhancement of −10 dB impedance bandwidth of DRA. Besides, a dielectric resonator-above-patch (DRAP),[58] resulting in the improvement of impedance bandwidth from 5.8% to 29.2%. The relevant outcomes in terms of impedance bandwidth, efficiency, modes, and gain

TABLE 4 CP techniques DRA at mm-wave applications

Ref.	DRA	Feeding	ε_r	f_o (GHz)	CP BW	Modes	Gain (dB)
46	Rect.	Aperture	10.2	55.8-65.2	56.5-63.5	$HEM_{15\delta}$	13.2
50	Rect.	Aperture	10.2	20.5-24.3 26.1-30.4	21.2-24.1 27.4-28.8	TE_{111} TE_{113}	5 8
35	Rect.	SIW	20.5	24.8-31.2	24-32.2	NM	18.3
51	Rect.	Aperture	NM	27-31.8	29.7-30	TE^{x}_{111},TE^{y}_{111}	12.7
36	Rect.	Aperture	10.2, 6.15, 2.2	58-68	~ 60-63	NM	11
52	Cyli.	Aperture	10.2	57-64	55-64.5	$HEM_{11\delta}$	11.43
41	Rect.	Aperture	10.2	29-31.5	29.7-30.6	NM	15.5

Note: ~ is estimated from the graph.

Abbreviations: CP BW, circular polarization bandwidth; Cyli., cylindrical; f_o, operating frequency; NM, not mentioned; Rect., rectangular; Ref., reference; ε_r, dielectric constant of DR.

of bandwidth enhancement techniques at mm-wave applications are tabulated in Table 5.

In Tables 3–5, a detailed state-of-the-art DRAs at mm-wave frequency band is studied, in correlation with the gain enhancement, attainment of circular polarization and bandwidth enhancement. For some of the cases, it is observed that empirical formulae and their mode analysis are not investigated except rectangular and cylindrical shaped DRAs. So, in this review article, by studying antenna parameters, empirical formulae are derived for hexagonal and octagonal shaped DRAs. Subsequently, mode analysis is persuaded for cylindrical, rectangular, hexagonal, and octagonal DRAs by the help of electric field and magnetic field distribution at 60 GHz mm-wave frequency band. In addition, commonly used DR with substrate materials and their potential applications are also reported in this article.

4 | IMPLEMENTATION OF DIFFERENT SHAPED DRAs AT 60 GHz FREQUENCY BAND

In the previous section, a complete technical insight about DRAs at the mm-wave frequency band is presented.[59] Here, different shaped DRAs such as cylindrical, rectangular, hexagonal, and octagonal at 60 GHz are designed, implemented, and analyzed using CST microwave studio. It is characterized by the performance index of antenna parameters such as impedance bandwidth, input impedance response, realized gain, radiation efficiency and normalized radiation pattern, and mode analysis at 60 GHz frequency band. In addition, commonly used DR with substrate materials and their potential applications at mm-wave communications are also reported. The design of different shaped DRAs is based upon the same substrate dimensions with the same value

TABLE 5 Bandwidth enhancement of DRAs at mm-wave applications

Ref.	DRA	Feeding	ε_r	f_o (GHz)	Eff. (%)	Mode	Gain (dB)
54	Rect.	Aperture	2.5, 4	56.5-63.5	90	NM	10.5
31	Rect.	SIW	2.5	29.3-35.2	76	NM	12
55	Cube	Microstrip	40	54.5-63 58.5-62	NM	NM	5 6
56	Rect.	Bond wire	11.9	52.8-65	74	TE^{x}_{111},TE^{y}_{111}	4.5
57	Rect.	SIW	10.2	31-40	NM	TE^{y}_{111}	4.6
58	Rect.	CPW	12.9	54-71.5	NM	TE_{111}	3.6

Abbreviations: Eff., efficiency; f_o, operating frequency; NM, not mentioned; Rect., rectangular; Ref., reference; ε_r, dielectric constant of DR.

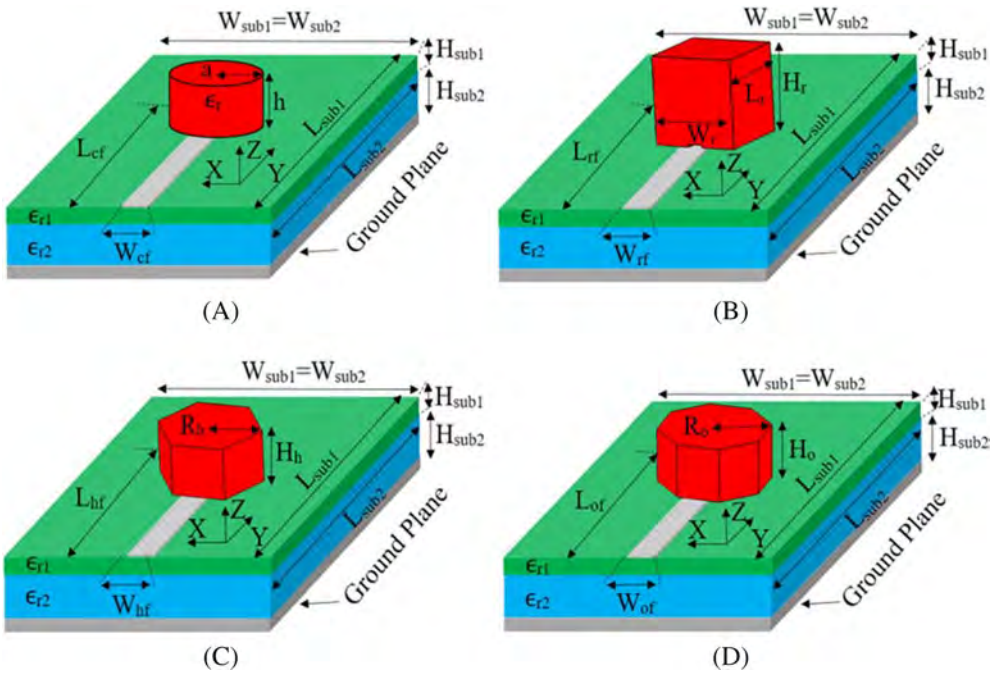

FIGURE 3 Different shapes of DRA at 60 GHz mm-wave applications. A, CDRA; B, RDRA; C, HDRA; D, ODRA (optimized dimensions: $L_{sub1} = L_{sub2} = 1.6$, $W_{sub1} = W_{sub2} = 1.6$, $H_{sub1} = 0.022$, $H_{sub2} = 0.3$, $a = 0.332$, $h = H_h = H_o = 0.312$, $L_{cf} = L_{rf} = L_{hf} = L_{of} = 1.12$, $W_{cf} = W_{cf} = W_{hf} = W_{of} = 0.1$, $L_r = W_r = H_r = 0.575$, $\varepsilon_{r1} = 4$, $\varepsilon_{r2} = 11.9$, All dimensions are in mm). CDRA, cylindrical DRA; DRA, dielectric resonator antenna; HDRA, hexagonal DRA; RDRA, rectangular DRA; ODRA, octagonal DRA

TABLE 6 A comparative study of different shaped DRAs at 60 GHz mm-wave band

	Different shaped DRA			
Parameters	**Cylindrical DRA**	**Rectangular DRA**	**Hexagonal DRA**	**Octagonal DRA**
Optimized dimensions of DRA (mm)	$a = 0.332$ $h = 0.312$	$L_r = W_r = H_r = 0.575$	$R_h = 0.332$ $H_h = 0.312$ $L_h = 0.332$	$R_o = 0.332$ $H_o = 0.312$ $L_o = 0.25$
Dimensions in term of λ	$a = 0.0664\lambda$ $h = 0.062\lambda$	$L_r = W_r = H_r = 0.115\lambda$	$R_h = 0.0664\lambda H_h = 0.062\lambda$ $L_h = 0.0664\lambda$	$R_o = 0.0664\lambda$ $H_o = 0.062\lambda$ $L_o = 0.05\lambda$
Surface area of DR (mm^2)	0.346	0.330	0.286	0.311
Volume of DR (mm^3)	0.107	0.190	0.089	0.097
Path length (mm)	2.08	2.3	1.98	2
−10 dB Impedance bandwidth (GHz)	52.7-62.8	57-62.2	55.8-64.6	54.2-63.5
Directivity (dBi)	5.03	5.09	4.81	4.89
Antenna efficiency (%)	97.2	97.8	96.2	97.7
Gain (dB)	4.9	4.99	4.63	4.76
Mode	HEM_{111}	TE_{111}	HEM_{111}	HEM_{111}

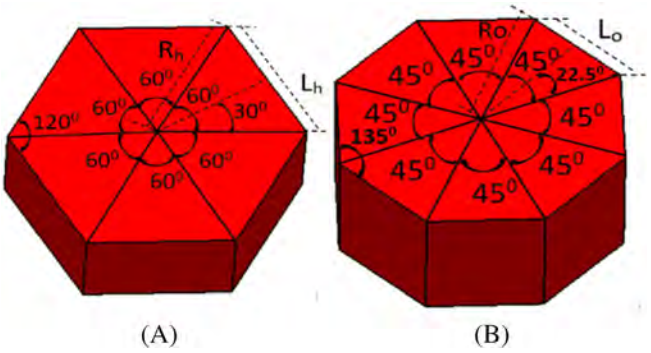

FIGURE 4 Structure of A, HDRA and B, ODRA from CDRA. CDRA, cylindrical DRA; HDRA, hexagonal DRA; ODRA, octagonal DRA

of permittivity shown in Figure 3. The ideology behind the proposed antenna is to enhance the impedance bandwidth using a double-layered substrate with different permittivity along with a simple microstrip feed transmission line. Typically, surface wave increases with the increase in substrate thickness. This leads to an increase in impedance bandwidth. In the case of the microstrip patch antenna, such geometrical sequences result in a decrease in system efficiency. However, here, antenna efficiency is higher than 95%, due to presence of DR, which is much more than the printed antennas. The proposed antennas cover the spectrum of 60 GHz mm-wave communications.[59]

4.1 | Antenna geometry

4.1.1 | Cylindrical DRA and rectangular DRA

The proposed antenna consists of DR ($Ca_5Nb_2TiO_{12}$) with a permittivity (ε_r) of 48, placed on a silicon layer substrate ($\varepsilon_{r1} = 4$) with dimensions of 1.6 (L_{sub1}) × 1.6 (W_{sub1}) × 0.022 (H_{sub1}) mm^3; with another silicon layer substrate ($\varepsilon_{r2} = 11.9$) with dimension of 1.6 (L_{sub2}) × 1.6 (W_{sub2}) × 0.3 (H_{sub2}) mm^3 as shown in Figure 3. It is fed by a 50-Ω microstrip line, having optimized dimensions of feed width ($W_{cf} = W_{rf}$) 0.1 mm placed on top of silicon layer substrate. The dimension of feed width for double-layer substrate with different permittivity is calculated by using microstrip transmission line Equations (5) and (6) as follows:

$$Z_0 = \left\{ \frac{120\pi}{\sqrt{\epsilon_{\text{eff}}}} \times \left(\frac{1}{\left(\frac{w}{h} + 1.393 + 0.677 \times \ln\left(\frac{w}{h} + 1.444\right)\right)} \right) \right. \tag{5}$$

where,

$$\epsilon_{\text{eff}} = \left\{ \frac{\epsilon_{r,\text{sub}} + 1}{2} + \frac{\epsilon_{r,\text{sub}} - 1}{2} \left[\frac{1}{\sqrt{1 + \frac{12h}{w}}} \right] \right.$$

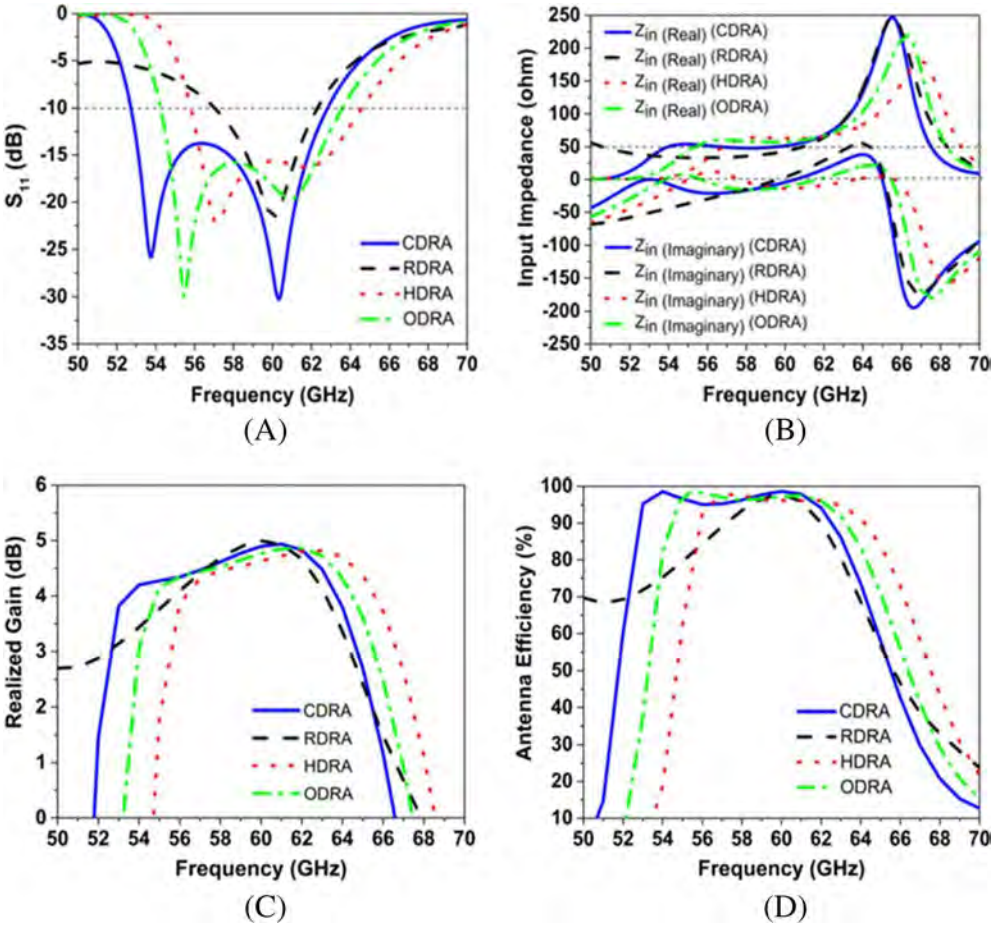

FIGURE 5 Simulated outcomes of different shaped DRAs at 60 GHz: A, S_{11} vs frequency; B, input impedance vs frequency; C, realized gain vs frequency; and D, antenna efficiency vs frequency. DRA, dielectric resonator antenna

For the double-layered substrate, the permittivity is calculated by using static capacitance model[60] in the following Equation (6).

$$\in_{r,sub} = \frac{H_{eff,sub}}{\frac{H_{sub1}}{\in_{r1}} + \frac{H_{sub2}}{\in_{r2}}} \tag{6}$$

where,

$$H_{eff,sub} = H_{sub1} + H_{sub2}$$

The dimension of DR at a given resonant frequency of modes ($f_{res\,(HEM_{111})}$ and $f_{res\,(TE_{111})}$) are calculated using empirical formulae in Equations (1) and (2) and the optimized dimensions are tabulated in Table 6.

4.1.2 | Hexagonal DRA and octagonal DRA

Hexagonal and octagonal DR structures are derived from cylindrical DR structure. Parameters like the dimensions of dual silicon layer substrate and height of the DR with permittivity remain the same with the previous value, as shown in Figure 3. Mathematically, hexagonal DRA (HDRA) is obtained by connecting six equilateral triangles side by side, each of them having a side length (L_h) of 0.332 mm, as shown in Figure 4A and is calculated by Equation (7). Similarly, octagonal DRA (ODRA) is obtained by connecting eight triangles side by side, each of them having a side length (L_o) of 0.25 mm as shown in Figure 4B. It is calculated on the basis of Equation (8).

$$L_h = 2R_h \sin 30^0, R_h = \frac{L_h}{2\sin 30^o} = L_h \tag{7}$$

$$L_o = 2R_o \sin 22.5^0, R_o = \frac{L_o}{2\sin 22.5^0} = 1.3L_o \tag{8}$$

To calculate their resonant frequency, empirical formulae are developed for HDRA & ODRA, with due consideration of parameters such as R_o, H_h, R_h, H_o, H_h, and ε_r, as shown in the Equations (7) and (8), respectively. Their validation is dependent upon the S_{11} vs frequency characteristics of HDRA and ODRA, resonating at 60 GHz operating frequency. In the case of hexagonal shape DRA, the resonant

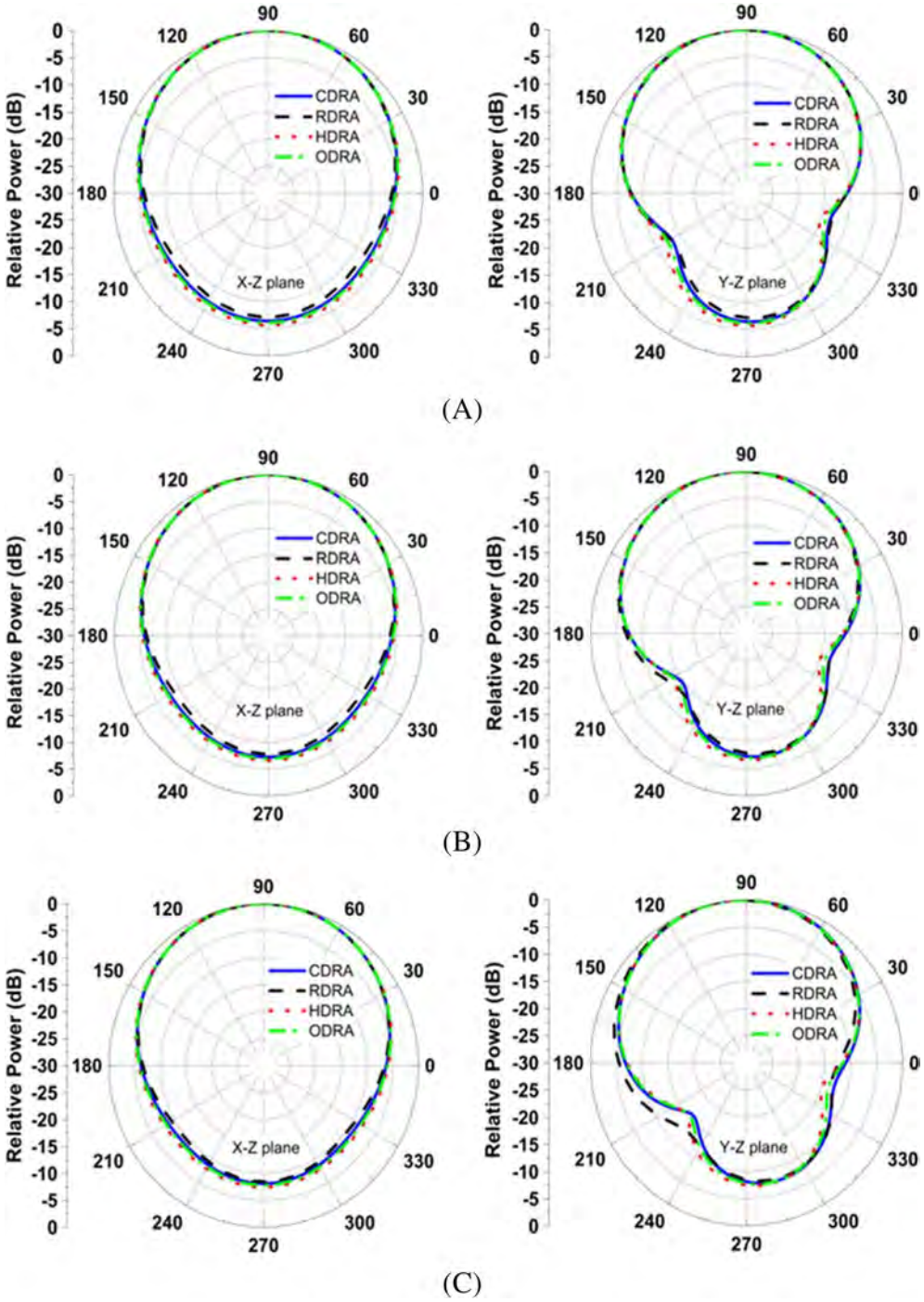

FIGURE 6 Normalized radiation pattern of different shaped DRAs in the X-Z plane and Y-Z plane at A, 58 GHz; B, 60 GHz; C, 62 GHz. DRA, dielectric resonator antenna

frequency of HEM_{111} mode can be calculated by using Equation (9).

$$f_{\text{res (HEM}_{111})} = \frac{6.324c}{2\pi R_{\text{h}}\sqrt{\epsilon_{\text{eff}}+2}}\left[0.27+0.36\left(\frac{R_{\text{h}}}{4H_{\text{h}}}\right)+0.02\left(\frac{R_{\text{h}}}{4H_{\text{h}}}\right)^2\right] \quad (9)$$

Similarly, for octagonal shape DRA, the resonant frequency of HEM_{111} mode can be calculated by using Equation (10).

$$f_{\text{res (HEM}_{111})} = \frac{6.324c}{2\pi R_{\text{o}}\sqrt{\epsilon_{\text{eff}}+2}}\left[0.27+0.36\left(\frac{R_{\text{o}}}{4H_{\text{o}}}\right)+0.02\left(\frac{R_{\text{o}}}{4H_{\text{o}}}\right)^2\right] \quad (10)$$

4.2 | Simulated results and discussions

The S_{11} response of the different shaped DRAs is shown in Figure 5A. The simulated S_{11} are 52.7 to 62.8 GHz for

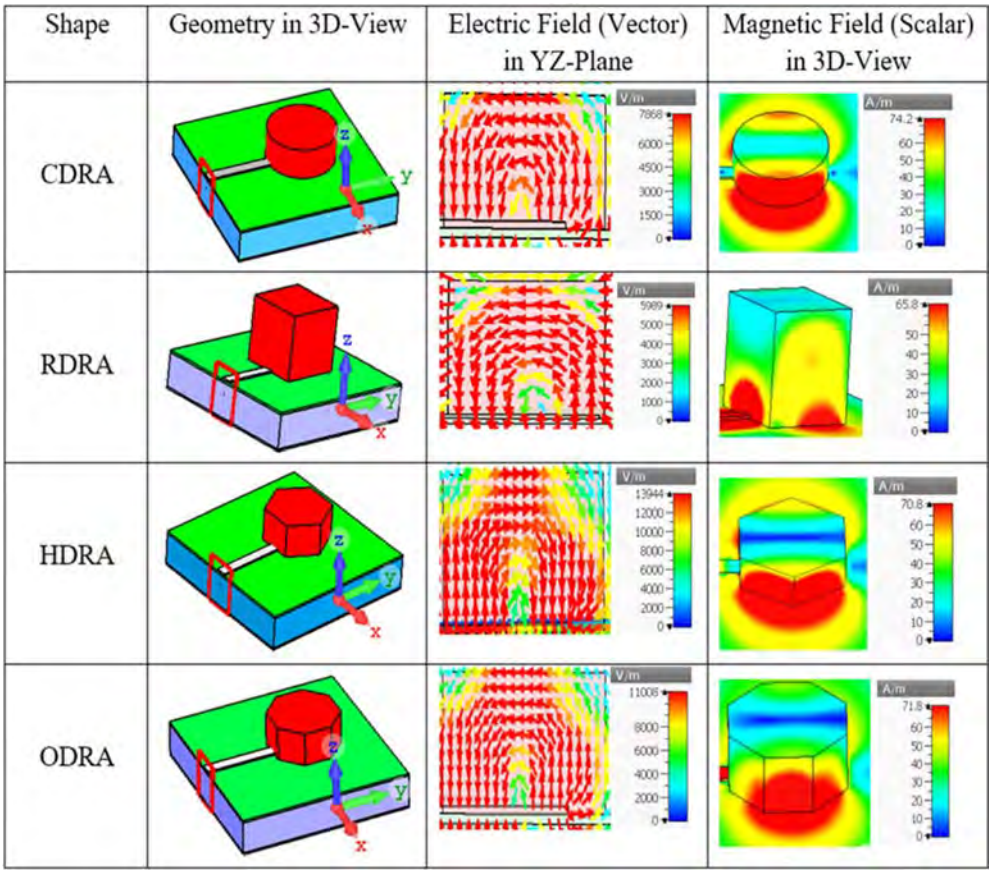

FIGURE 7 Electric field and magnetic field distributions of different shaped DRAs at 60 GHz. DRAs, dielectric resonator antennas

CDRA, 57 to 62.2 GHz for RDRA, 55.8 to 64.6 GHz for HDRA, and 54.2 to 63.5 GHz for ODRA. We observed from the simulated S_{11} graph, the bandwidth is directly proportional to the path length of DR. Due to the large path length, the bandwidth of CDRA is more than HDRA and ODRA. Consequently, shifting of bandwidth to the higher band is inversely proportional to the surface area of DR. During the comparison, CDRA, HDRA, and ODRA are taken into consideration, because HDRA and ODRA are derived from CDRA structure. The input impedance response vs frequency of the different shaped DRAs are shown in Figure 5B. It can be observed that, within the operating frequency range, the real part of the impedance is nearly to 50-Ω while the imaginary part lies nearly 0-Ω, respectively. As a result, different shaped DRAs are perfectly matched between microstrip feed and DR. The realized gain is 4.89 dB for CDRA, 4.97 dB for RDRA, 4.63 dB for HDRA, and 4.76 dB for ODRA at 60 GHz frequency with antenna efficiency of above 95% within the operating frequency band as shown in Figure 5C,D. All the relevant outcomes are shown in Table 6. The normalized radiation pattern for different shaped DRAs at 58, 60, and 62 GHz is illustrated in Figure 6. With reference to the graph in X-Z and Y-Z plane, the radiation patterns are broadside in nature and also following the same pattern without instability.

4.3 | Analysis of modes

To highlight the theoretical insight about DRAs, modal analysis is performed and it is validated through electric and magnetic field distribution[27,61,62] with the help of EM solver, as shown in Figure 7. The hybrid electromagnetic mode: HEM_{111} or $HEM_{11\delta}$ is observed in CDRA, HDRA, and ODRA, where both electric fields and magnetic fields are in the direction of propagation. In this mode ($HEM_{11\delta}$), the first subscript indicates the number of full-period fields variation along azimuthal direction or number of half-wave field pattern around half circumference of the top view of DR. Similarly, second subscript indicates the number of half-wave fields and its variation along the radius, that is, in-between center and periphery of the structure and last subscript (δ) indicates the number of half-wave fields variation in the direction of propagations. Similarly, in the case of RDRA, TE_{111} mode is observed and it indicates that the number of half-wave field variations occurs in the direction of the X-axis, Y-axis, and Z-axis (direction of propagation), respectively.

TABLE 7 DR and substrate materials with their potential applications at millimeter-wave DRAs

Ref. no	Substrate material	DR material	Potential applications
27	Arlon 25 N	Green tape 9K7	• 5G & small cell concept • Metro network service • High definition (HD) video • IEEE 802.11ad WiGig (Wireless gigabit alliance) • Satellite communication • Automotive application • Body scanners • Radar • Medical application • Virtual reality headsets
28	Roger RT/5870	Roger RT/6010	
30	Composite material [PREPERM TP20280]	Composite material [PREPERM TP20280]	
31	Rogers 6006	Rogers 6010, 6006, 5880	
32	Rogers RT 5880	Rogers RT 6010	
33	Rogers RT 5880	Rogers RT 6010	
34	Rogers RT 5880	Rogers RT 5880	
35	Rogers RT5880	Ceramic material	
36	Rogers 6010, 6006, 5880	Rogers 6006	
39	Rogers 5880, Rogers 6010	Rogers RT6010	
41	Rogers 3006	Rogers RT6010	
43	Rogers RT 6002	Rogers RT6010	
44	Silicon wafer	Silicon wafer	
45	Rogers RT 5870	Rogers RT6010	
47	Rogers RT 6002	Rogers TMM6	
49	Silicon-based IPD	High resistivity silicon	
50	Rogers 3010	Rogers 5880	
57	Rogers RT5880	Rogers RT6010	
[PP]	Silicon layer	$Ca_5Nb_2TiO_{12}$	

Abbreviations: PP., present paper; Ref., reference.

5 | DR MATERIALS AND POTENTIAL APPLICATION OF MILLIMETER-WAVE DRAs

The material properties of dielectric and substrate of DRAs play a crucial role for antenna designers. These properties influence antenna characteristics such as operating frequency, impedance bandwidth, quality factor (Q-factor), antenna gain, and antenna radiation efficiency. In addition to that, dielectric material losses also directly impact the antenna characteristics, because material losses depend on the permittivity of the dielectric material.

Thus, this part will allow the antenna designer to choose the perfect material for DR and substrate, to design the millimeter-wave DRAs. Material used for millimeter-wave DRAs are presented in Table 7. Due to ultra-high data rate transmission, nowadays, research on DRAs in the millimeter-wave applications are going to increase in a faster manner. It is possible to send the information between cell phones and satellites at a faster rate, that is, nearly 10 to 20 times (10-20 gigabit per second) faster than standard 4G networks (1 gigabit per second) because millimeter- wave can support ultra-high-speed data rate due to higher bandwidth. The potential applications of millimeter-wave DRAs are reported in Table 7.

6 | CONCLUSION

The purpose of this article is to provide a technical review of the development of DRAs at mm-wave communication. It starts with a general overview of the basic configuration of DRAs. Then, state-of-the-art development of different techniques specifically used for enhancement of gain, generation of circular polarization, and improvement of impedance bandwidth at mm-wave frequency are highlighted. At last, different shaped DRAs such as CDRA, RDRA, HDRA, and ODRA at 60 GHz are implemented by using CST microwave studio. The proposed antenna consists of a dual silicon substrate having different permittivity (double-layered structure) used for the enhancement of impedance bandwidth. The −10 dB impedance bandwidth is found to be from 52.7 to 62.8 GHz, 57 to 62.2 GHz, 55.8 to 64.2 GHz, and 54.2 to

63.5 GHz. Subsequently, empirical formulae are developed for HDRA and ODRA at 60 GHz frequency band. Finally, the analysis is concluded with the study of modes along with the DR materials and potential applications. Hybrid electromagnetic modes, that is, HEM_{111} is observed for CDRA, HDRA, and ODRA. Similarly, in the case of RDRA, TE_{111} is observed form the structure of DR. In correspondence to its utility as a review article for mm-wave DRAs, a detailed analogy regarding the design of different shaped DRAs along with their mode analysis, is presented to benefit the readers.

ORCID

Priya R. Meher https://orcid.org/0000-0002-0918-9618
Bikash R. Behera https://orcid.org/0000-0001-8312-4022
Sanjeev K. Mishra https://orcid.org/0000-0002-9089-9763

REFERENCES

1. Petosa A, Ittipiboon A. Dielectric resonator antennas: a historical review and the current state of the art. *IEEE Antennas Propag Mag*. 2010;52(5):91-116.
2. Richtmyer RD. Dielectric resonators. *J Appl Phys*. 1939;10(6):391-398.
3. Long SA, Mcallister MWM, Shen LC. The resonant cylindrical dielectric cavity antenna. *IEEE Trans Antennas Propag*. 1983;31(3):406-412.
4. Kumar G, Ray KP. *Broadband Microstrip Antennas*. Norwood, MA: Artech House; 2003.
5. Liu H, Li Z, Sun X. Compact defected ground structure in microstrip technology. *Electron Lett*. 2005;41(3):132-134.
6. Ghosh D, Ghosh SK, Chattopadhyay S, et al. Physical and quantitative analysis of compact rectangular microstrip antenna with shorted non-radiating edges for reduced cross-polarized radiation using modified cavity model. *IEEE Antennas Propag Mag*. 2014;56(4):61-72.
7. Ullah U, Ain MF, Ahmad ZA. A review of wideband circularly polarized dielectric resonator antennas. *China Commun*. 2017;14(6):65-79.
8. Dash SKK, Khan T, Antar YMM. A state of art review on performance improvement of dielectric resonator antennas. *Int J RF Microw Comput Aid Eng*. 2018;28(6):1-19.
9. Chowdhury R, Mishra N, Sani MM, Chaudhary RK. Analysis of a wideband circularly polarized cylindrical dielectric resonator antenna with broadside radiation coupled with simple microstrip feeding. *IEEE Access*. 2017;5:19478-19485.
10. Keyrouz S, Caratelli D. Dielectric resonator antennas: basic concepts, design guidelines and recent developments at millimeter-wave frequencies. *Int J Antennas Propag*. 2016;2016:1-20.
11. Mongia RK, Bharatia P. Dielectric resonator antennas-a review and general design relations for resonant frequency and bandwidth. *Int J RF Microw Comput Aid Eng*. 1994;4(3):230-247.
12. Moon JJ, Park SO. Dielectric resonator antenna for dual-band PCS/IMT-2000. *Electron Lett*. 2000;36(12):1002-1003.
13. Legier JF, Kennis P, Toutain S, Citerne J. Resonant frequencies of rectangular dielectric resonators. *IEEE Trans Microw Theory Techn*. 1980;28(9):1031-1034.
14. Makwana GD, Vinod KJ. Design of a compact rectangular dielectric resonator antenna at 2.4 GHz. *Progr Electromagn Res C*. 2009;11:69-79.
15. Luk KM, Leung KM, Lin D. Analysis of hemispherical dielectric resonator antenna. *Radio Sci*. 1993;28(6):1211-1218.
16. Mukherjee B, Patel P, Reddy GS, Mukherjee J. A novel hemispherical dielectric resonator antenna with array of slots for wideband applications. *Progr Electromagn Res C*. 2013;36:207-221.
17. Mcallister MW, Long SA. Resonant hemispherical dielectric resonator antenna. *Electronics Lett*. 1984;20(16):657-659.
18. Hamsakutty V, Kumar AVP, Yohannan J, Mathew KT. Coaxial fed hexagonal dielectric resonator antenna for circular polarization. *Microw Opt Technol Lett*. 2006;48(3):581-582.
19. Dash SKK, Khan T, Kanuajia BK. Conical dielectric resonator antenna with improved gain and bandwidth for X-band applications. *Int J Microw Wirel Technol*. 2017;9(8):1-8.
20. Ittipiboon A, Mongia RK, Antar YMM, Bharatia P, Cuhaci. Aperature fed rectangular and triangular dielectric resonators for use as magnetic dipole antennas. *Electron Lett*. 1993;29(23):2001-2002.
21. Kishk AA. A triangular dielectric resonator antenna excited by a coaxial probe. *Microw Opt Technol Lett*. 2001;30(5):340-341.
22. Pan Y, Leung KW. Wideband circularly polarized trapezoidal dielectric resonator antenna. *IEEE Antenna Wirel Propag Lett*. 2010;9:588-591.
23. Matin MA. Review on millimeter-wave antenna potential candidate for 5G enable applications. *Adv Electromagn*. 2016;5(3):98-105.
24. Alhalabi RA, Chiou YC, Rebeiz GM. Self-shielded high-efficiency yagi-Uda antennas for 60 GHz communications. *IEEE Trans Antennas Propag*. 2011;59(3):742-750.
25. Kramer O, Djerafi T, Wu K. Very small footprint 60 GHz stacked yagi antenna array. *IEEE Trans Antennas Propag*. 2011;59(9):3204-3210.
26. Sun M, Qing X, Chen ZN. 60-GHz end-fire fan-like antennas with wide beamwidth. *IEEE Trans Antennas Propag*. 2013;61(4):1616-1622.
27. Mrnka M, Cupal M, Raida Z, Pietrikova A, Kocur D. Millimetre-wave dielectric resonator antenna array based on directive LTCC elements. *IET Microw Antennas Propag*. 2018;12(5):662-667.
28. Abdel-Wahab WM, Safavi-Naeini S, Busuioc D. High gain/ efficiency 2D-dielectric resonator antenna array for low-cost mm-wave systems. Paper presented at: 2011 IEEE International Symposium on Antennas and Propagation (APSURSI), Spokane; 2011:1682-1684.
29. Zandieh A, Abdellatif AS, Taeb A, Safavi-Naeini S. High resistivity silicon DRA array for millimeter-wave high gain applications. Paper presented at: 2017 IEEE MTT-S International Microwave Symposium (IMS), Honololu; 2017:857-860.
30. Zhang S. Three-dimensional printed millimeter-wave dielectric resonator reflectarray. *IET Microw Antennas Propag*. 2017;11(14):2005-2009.
31. Mazhar W, Klymyshyn DM, Wells S, Qureshi AA, Jacobs M, Achenbach S. Low-profile grid dielectric resonator antenna for

mm-wave applications. *IEEE Trans Antennas Propag*. 2019;67 (7):4406-4417.
32. Gong K, Hu XH, Hu P, Deng BJ, Tu YC. A series-fed linear substrate integrated dielectric resonator antenna array for millimeter-wave applications. *Int J Antenna Propag*. 2018;2018: 1-6.
33. Deng BJ, Gong K, Hu XH, Wang P, Tu YC. 4×2 substrate integrated dielectric resonator antenna array in Ka-band. Paper presented at: IEEE Asia-Pacific Conference on Antennas and Propagation; 2018; Auckland, New Zealand:429-430.
34. Ashraf N, Vettlkalladi, Alkanhal AS. A DR loaded substrate integrated waveguide antenna for 60 GHz high-speed wireless communication system. *Int J Antenna Propag*. 2014;1-9.
35. Sun W-J, Yang W-W, Qin W, Tang H, Chen J-X. Design of a circularly polarized dielectric resonator antenna array for millimeter-wave applications. Paper presented at: IEEE MTT-S International Wireless System Symposium; 2019; Guangzhou, China:1-3.
36. Laribi M, Hakem N, Elkarkraoui T. Hight-gain circularly polarized multilayer dielectric resonator antenna for millimeter-wave application. Paper presented at: 2017 IEEE International Symposium on Antennas and Propagation & USNC/URSI National Radio Science Meeting; 2017; San Diego:1523-1524.
37. Chatla AB, Bandyopadhyay S, Maji B. A dual-band z-shape stepped dielectric resonator antenna for millimeter-wave applications. *Recent Development in Wireless Sensor and Ad-Hoc Networks-Signals and Communication Technology*. Springer; 2015:103-124.
38. Perron A, Denidni TA, Sebak A. High-gain hybrid dielectric resonator antenna for millimeter-wave applications: design and implementation. *IEEE Trans Antennas Propag*. 2009;57(10): 2882-2892.
39. Perron A, Denidni TA, Sebak AR. Circularly polarized microstrip/elliptical dielectric ring resonator antenna for millimeter-wave applications. *IEEE Antennas Wirel Propag Lett*. 2010;9: 783-786.
40. Al-Hasan MJ, Denidni TA, Sebak A. EBG dielectric-resonator antenna with reduced back radiation for millimeter-wave applications. Paper presented at: Proceedings of the 2012 IEEE International Symposium on Antennas and Propagation; 2012; Chicago: 1-2.
41. Akbari M, Gupta S, Farahani M, Sebak AR, Denidni TA. Gain enhancement of circularly polarized dielectric resonator antenna based on FSS superstrate for MMW applications. *IEEE Trans Antennas Propag*. 2016;64(12):5542-5546.
42. Coulibaly Y, Nedil M, Talbi L, Denidni TA. Design of high gain and broadband antenna at 60 GHz for underground communications systems. *Int J Antenna Propag*. 2012;1-7.
43. Kesavan A, Mantash M, Denidni TA. Beam-switching millimetre-wave antenna using cantilever-based FSSs. *IET Microw Antennas Propag*. 2018;12(13):2019-2024.
44. Sallam MO, Serry M, Sherif S, Shamim A, Raedt WD, Vandenbosch GAE. Micromachined on-chip dielectric resonator antenna operating at 60 GHz. *IEEE Trans Antennas Propag*. 2015;63(8):3410-3416.
45. Wahab WMA, Busuioc D, Safavi-Naeini S. Low-cost planar waveguide technology-based dielectric resonator antenna (DRA) for millimeter-wave applications: analysis, design, and fabrication. *IEEE Trans Antennas Propag*. 2010;58(8):2499-2507.
46. Elboushi A, Haraz OM, Sebak A, Denidni T. A new circularly polarized high gain DRA millimeter-wave antenna. Paper presented at: 2010 IEEE Antennas and Propagation Society International Symposium; 2010; Toronto:1-4.
47. Liang X, Yang D, Jin R, Geng J. A 60-GHz wideband dielectric resonator antenna with inclined radiation. Paper presneted at: 2012 IEEE International Workshop on Antenna Technology (iWAT); 2012; Tucson:124-127.
48. Song Y, Kang K, Tian Y, et al. A hybrid integrated high-gain antenna with an on-chip radiator backed by off-chip ground for system-on-chip applications. *IEEE Trans Compon Packag Manuf Technol*. 2017;7(1):114-122.
49. Lin TY, Chiu T, Chang YC, Chang DC, Yen MH, Chen CK, Lin MS. A dual-band millimeter-wave high-gain dielectric resonator antenna using vertical assembly technology. Paper presented at: 2017 IEEE CPMT Symposium Japan (ICSJ); 2017; Kyoto:131-132.
50. Liu Y, Jiao Y-C, Weng Z, Chen G. A novel millimeter-wave dual-band circularly polarized dielectric resonator antenna. *Int J RF Microw Comput Aid Eng*. 2019;29(10):1-7.
51. Chu H, Guo Y. A novel approach for millimeter-wave dielectric resonator antenna array designs by using the substrate integrated technology. *IEEE Trans Antennas Propag*. 2017;65(2): 909-914.
52. Sun Y, Leung KW. Circularly polarized substrate-integrated cylindrical dielectric resonator antenna array for 60 GHz applications. *IEEE Antennas Wirel Propag Lett*. 2018;17(8):1401-1405.
53. Ahmad Z, Hesselbarth J. On-chip dual-polarized dielectric resonator antenna for millimeter-wave applications. *IEEE Antennas Wirel Propag Lett*. 2018;17(10):1769-1772.
54. Qureshi AA, Klymyshn DM, Tayfeh M, Mazhar W, Borner M, Mohr J. Template-based dielectric resonator antenna arrays for millimeter-wave applications. *IEEE Trans Antennas Propag*. 2017;65(9):4576-4584.
55. Rashidian A, Shafai L. Low-profile dielectric resonator antennas for millimeter-wave applications. Paper presented at: 15th International Symposium on Antenna Technology and Applied Electromagnetics; *2012*; Toulouse:1-2.
56. Lin TA, Chiu T, Chang DC. V-band dual-polarised square DRA with bond wire feeding structures. *Electron Lett*. 2017;53(12): 764-766.
57. Tu CY, Ma DD, Liu Y, Hu XH, Gong K. Broadband substrate integrated dielectric resonator antenna for millimeter-wave applications. Paper presented at: IEEE MTT-S International Microwave Workshop Series on Advanced Materials and Processes for RF and THz Applications (IMWS-AMP); 2016; Chengdu:1-3.
58. Oh J, Baek T, Shin D, Rhee J, Nam S. 60-GHz CPW-fed dielectric-resonator-above-patch (DRAP) antenna for broadband WLAN applications using micromachining technology. *Microw Opt Technol Lett*. 2007;49(8):1859-1861.
59. Meher PR, Behera BR, Mishra SK. Design of different shaped DRAs for 60 GHz millimeter-wave applications. Paper presented at: IEEE Indian Conference on Antenna and Propagation, India; 2018:1-4.
60. Petosa A, Simons N, Siushansian R, Ittipiboon A, Cuhaci M. Design and analysis of multisegment dielectric resonator antennas. *IEEE Trans Antennas Propag*. 2000;48(5):738-742.

61. Guha D, Banerjee A, Kumar C, Antar YMM. Higher-order mode excitation for high-gain broadside radiation from cylindrical dielectric resonator antennas. *IEEE Trans Antennas Propag*. 2012;60(1):71-77.
62. Kiran DV, Sankaranarayanan D, Mukherjee B. Compact embedded dual-element rectangular dielectric resonator antenna combining Sierpinski and Minkowski fractals. *IEEE Trans Compon Packag Manuf Technol*. 2017;7(5):786-791.

AUTHOR BIOGRAPHIES

Priya R. Meher received MTech degree with specialization in communication System Department of Electronics and Communication Engineering from GIET University, Gunupur, Odisha, India in 2015. He is currently pursuing PhD in RF and Microwaves, Department of Electronics and Telecommunication Engineering with International Institute of Information Technology Bhubaneswar, Odisha, India. Mr Meher has authored and co-authored in more than eight papers, in reputed conferences and journals. His research interests are wideband dielectric resonator antenna, wireless body area network antenna, RF-energy harvesting systems, and nanophotonics. Mr Meher is a student member of IEEE. (Email: priya.r.meher@ieee.org, c117008@iiit-bh.ac.in)

Bikash R. Behera received ME degree with specialization in Wireless Communication, Department of Electronics and Communication Engineering from Birla Institute of Technology Mesra, Ranchi, Jharkhand, India in 2016. He is currently pursuing PhD in RF and Microwaves, Department of Electronics and Telecommunication Engineering with International Institute of Information Technology Bhubaneswar, Odisha, India. In 2017, he is the recipient of Young Scientist Award at URSI-RCRS'17, Tirupati, India. He has authored and co-authored in more than 25 papers in reputed conferences and journals. His research interests are RF energy harvesting systems, metamaterials-inspired antenna designing, and the study of EM based optimization techniques. Mr Behera is a student member of IEEE. (Email: bikash.r.behera@ieee.org, c117004@iiit-bh.ac.in)

Dr Sanjeev K. Mishra (SM'16) has received PhD degree from Department of Electrical Engineering from Indian Institute of Technology Bombay, Mumbai, India in 2012. At present, he is working as an assistant professor in Department of Electronics and Telecommunication Engineering with International Institute of Information Technology Bhubaneswar, Odisha, India. He has authored and co-authored in more than 70 papers in reputed journals and conferences. He has two patents and written book on planar antennas. Dr Mishra is a recipient of Young Scientist Award at APRASC'13, Taiwan. His research interests are RF and microwave circuits and system design; Microwave remote sensing and sensors and measurements. He is a senior member of IEEE and reviewer of *IEEE Antennas & Wireless Propagation Letters*, *IET Microwaves, Antenna & Propagation*, *Progress in Electromagnetic Research* etc., and a reviewer for research projects in Science & Engg. Research Board for Department of Science & Technology, Government of India. (Email: sanjeev@iiit-bh.ac.in)

How to cite this article: Meher PR, Behera BR, Mishra SK. Design and its state-of-the-art of different shaped dielectric resonator antennas at millimeter-wave frequency band. *Int J RF Microw Comput Aided Eng*. 2020;e22221. https://doi.org/10.1002/mmce.22221